Preprints of the 19th World Congress
The International Federation of Automatic Control
Cape Town, South Africa. August 24-29, 2014

Subthreshold Resonance Oscillation and Generation of Action Potential

Tatsuo Kitajima* **Zhonggang Feng****

**Malaysia-Japan International Institute of Technology, UTM, Kuala Lumpur, Malaysia (Tel: 6-03-2203-1233; e-mail:kitajima@ic.utm.my).*
*** Graduate School of Science and Engineering, Yamagata University, Yamagata, Japan (zhgfeng@yz.yamagata-u.ac.jp)}*

Abstract: Subthreshold resonance has been observed in many excitatory/inhibitory neurons in the brain. It is suggested that such resonance phenomenon plays an important role in behavioral or perceptual functions in animals. However its mechanism and role remains unknown. Subthreshold resonance oscillation observed in a neuron suggests that a neuron has the frequency selectivity for various external inputs given to the brain. By advances in physiological experimental techniques, various voltage-dependent channels are thought to be involved in the generation of these resonance oscillations. Among these channels, a persistent sodium channel and a hyperpolarization-activated cation channel are said to mediate the generation of the subthreshold resonance oscillation observed in entorhinal cortex neurons and hippocampal pyramidal neurons. In this proposal, we examine how the external inputs influence the generation of action potentials at the neuron model with a persistent sodium channel and a hyperpolarization-activated cation channel parameters by using computer simulations

. Furthermore, the role of DC bias current input in the neuron model is also discussed.

Keywords: subthreshold resonance oscillation, voltage-dependent ion channels, Hodgkin-Huxley like dynamics, action potential, DC bias current.

1. INTRODUCTION

Chirp current is alternate current whose frequency increases or decreases with time. When Chirp current is given to a neuron as an input, its membrane potential can take in some cases the maximum at a specific frequency, especially in a subthreshold level. This oscillation phenomenon, known as subthreshold resonance oscillation, has been found in many excitatory and/or inhibitory neurons in the brain. In the 1980s, Mauro et al. and Koch reported the subthreshold resonance oscillation in squid giant axon (Mauro et al., Koch). Since then, resonance phenomena have been observed in neurons in various brain regions, such as inferior olive (Lampl & Yarom), thalamus (Puil et al.), neocortex (Gutfreund et al.), entorhinal cortex (Dickson et al.), and hippocampal CA1 area (Narayanan & Johnston). These resonance oscillations indicate that neurons in the brain have characteristics of frequency selectivity, that is, band pass filter property. Although it is suspected that the frequency selectivity of neurons should play an important role in behavioural or perceptual functions in animals, their practical roles have not yet been clarified. Recently, Narayanan et al. reported that the subthreshold resonance oscillation is closely related to the synaptic plasticity, which is currently considered to be one of the foundations of learning and memory in our brain (Kitajima & Hara, Johnston et al.). So, it is very interesting and attractive to understand those oscillatory features in more detail in order to understand the mechanism of higher information processing functions in the brain, such as short-term memory and the working memory.

By advances of experimental techniques, it has been reported that various voltage-dependent channels such as slow non-inactivating K^+ channel (Gutfreund et al.), hyperpolarization-activated cationic channel (Narayanan & Johnston), and Ca^{+2}-dependent K^+ channels (Puil et al.) are involved in these resonance oscillations. It is also reported that there exist many types of Ca^{+2} channels in the cell body and/or dendritic spines (Hutcheon et al.) and the intracellular Ca^{2+} concentration plays an important role in synaptic plasticity such that LTP (long term potentiation) and LTD (long term depression) (Kitajima & Hara, Johnston et al.). Furthermore, Puil et al. reported that low-threshold Ca^{2+} channels are closely related to subthreshold resonance phenomena in thalamic neurons (Puil et al.). As the membrane of nerve cells is the lipid bilayer, it is usually treated as an *RC* electric circuit. We already reported that for a neuron model with a low-threshold Ca^{2+} channel and the Ca^{2+}-dependent K^+ channel, the model can be transformed into the equivalent *RLC* electrical circuit model and has some kind of inductive elements to mediate the subthreshold resonance oscillation (Kitajima & Feng). On the other hand, a persistent sodium channel and a hyperpolarization-activated cation channel are

said to mediate the subthreshold resonance oscillation observed in entorhinal cortex neurons and hippocampal pyramidal neurons (Dickson et al., Haas & White). We also reported that a neuron model with a persistent sodium channel and a hyperpolarization-activated cation channel has similar inductive elements (Kitajima).

As it is well known, neurons can generate action potentials whenever their membrane potentials exceed the threshold after a refractory period. That is, if the membrane potential of a neuron is under threshold, i.e. in a subthreshold level, its neuron cannot generate action potentials. The fact that a neuron has the subthreshold resonance property indicates that its membrane potential can take the maximum for alternatee current input with a specific frequency and might have a chance to generate action potentials. In this paper, we construct a compartmental neuron model with a persistent sodium channel and a hyperpolarization-activated cation channel into which well known Hodgkin-Huxley models are incorporated in order to generate action potentials. By using computer simulation, we examine how the external alternate current with various frequencies affects the generation of action potentials in this neuron model. Furthermore, the role of DC bias current input in the neuron model is also discussed.

2. COMPARTMENTAL NEURON MODEL

A compartmental neuron model includes a persistent sodium channel, N_{aP}, and a hyperpolarization-activated cation channel, H. This model also contains a sodium channel, N_a, and a delayed rectifier potassium channel, K, in order to generate the action potential. Fig.1 shows its electrical circuit model.

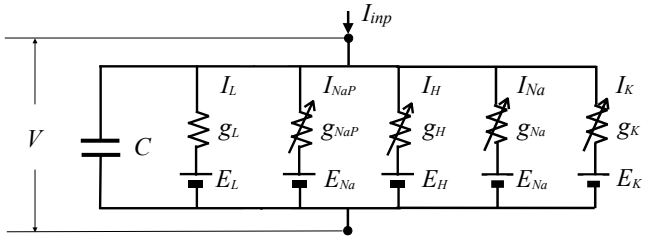

Fig.1. An electrical circuit of a compartmental neuron model. V is the membrane potential, C is the membrane capacitance, g_L is the leak conductance, g_{NaP}, g_H, g_{Na}, and g_K are channel conductances for N_{aP}, H, N_a, and K, respectively. E_L is the reversal potential. E_{Na}, E_K and E_h is an equilibrium potential for N_{aP} and N_a. E_K and E_H are equilibrium potentials for K and H. I_L is the leak current. I_{NaP}, I_H, I_{Na}, and I_K are the currents through N_{aP}, H, N_a, and K, respectively. I_{inp} is the synaptic input current.

The dynamics of this neuron model can be expressed by the following conductance-based Hodgkin-Huxley-like (HH-like) equations (Acker et al.):

$$C\,dV/dt = -I_L - I_{NaP} - I_h - I_{Na} - I_K + I_{inp}, \tag{1}$$

The leak current I_L is given by

$$I_{\mathrm{L}} = G_{\mathrm{L}}\,(V - V_r), \tag{2}$$

where G_{L} is the leak conductance and V_r is the resting potential. The current through *NaP* channel is given by

$$I_{NaP} = G_{NaP}\, m_{NaP}(V)\,(V - E_{Na}), \tag{3}$$

where G_{NaP} is the maximum amplitude of *NaP* channel conductance and the activation variable $m_{NaP}(V)$ satisfies the following equation:

$$dm_P(V)/dt = \{m_{P\infty}(V) - m_P(V)\}/\,\tau_{mP} \tag{4}$$

$$m_{P\infty}(V) = 1/\{1 + \exp(-(V+38)/6.5)\} \tag{5}$$

$$\tau_{mP} = 0.15 \text{ msec} \tag{6}$$

Similarly, the current through H channel is given by

$$I_h = G_h\,\{0.65\, m_{hf}(V) + 0.35\, m_{hs}(V)\}\,(V - E_h) \tag{7}$$

where G_h is the maximum amplitude of H channel conductance and activation variables $m_{hf}(V)$ and $m_{hs}(V)$ satisfy the following equations:

$$dm_{hf}(V)/dt = \{m_{hf\infty}(V) - m_{hf}(V)\}/\,\tau_{mhf} \tag{8}$$

$$m_{hf\infty}(V) = 1/\{1 + \exp((V+79.2)/9.78)\} \tag{9}$$

$$\tau_{mhf}(V) = 0.51/\{\exp((V-1.7)/10) + \exp((-(V+340)/52)+1\} \tag{10}$$

$$dm_{hs}(V)/dt = \{m_{hs\infty}(V) - m_{hs}(V)\}/\,\tau_{mhs} \tag{11}$$

$$m_{hs\infty}(V) = 1/\{1 + \exp((V+71.3)/7.9)\} \tag{12}$$

$$\tau_{mhs}(V) = 5.6/\{\exp((V-1.7)/14) + \exp((-(V+260)/43)+1\} \tag{13}$$

Furthermore, the current through *Na* channel is given by

$$I_{Na} = G_{NaP}\, m(V)^3\, h(V)\,(V - E_{Na}), \tag{14}$$

where G_{Na} is the maximum amplitude of *Na* channel conductance and the activation variable $m(V)$ and the inactivation variable $h(V)$ satisfy the following equations:

$$dm(V)/dt = \alpha_m(V)\,\{1 - m(V)\} - \beta_m(V)\,m(V) \tag{15}$$

$$\alpha_m(V) = 0.1\,(23 + V)\{1 - \exp(-(23+V)/10)\} \tag{16}$$

$$\beta_m(V) = 4\,\exp(-(V+48)/18) \tag{17}$$

$$dh(V)/dt = \alpha_h(V)\,\{1 - h(V)\} - \beta_h(V)\,h(V) \tag{18}$$

$$\alpha_h(V) = 0.07\,\exp(-(V+37)/20) \tag{19}$$

$$\beta_h(V) = 1/\{\exp(-(V+7)/10) + 1\} \tag{20}$$

Similary, the current through K channel is given by

$$I_K = G_K\, n(V,t)^4\,(V - E_K) \tag{21}$$

where G_K is the maximum amplitude of K channel conductance and the activation variable $n(V)$ satisfies the following equation:

$$dn(V)/dt = \alpha_n(V)\ \{1-n(V)\} - \beta_n(V)\, n(V) \quad (22)$$

$$\alpha_n(V) = 0.01\ (V+27)\{1-\exp(-(V+27)/10)\} \quad (23)$$

$$\beta_n(V) = 0.125\ \exp(-(V+37)/80) \quad (24)$$

As the frequency of the input current is increasing as time passes, the input current I_{inp} is given by

$$I_{inp} = A_{inp}\ \sin(\omega(t))\ t\ ) + id, \quad \omega(t) = 2\ \pi f\, t\ /T, \quad (25)$$

where id is DC bias current and T is a period in which the frequency spans linearly from zero to f.

3. COMPUTER SIMULATIONS

Parameters and constants used in computer simulations through whole this chapter are determined by referring to papers by Gutfreund et al., Kitajima & Hara, and Acker et al.. Those basic values are shown in Table 1. Table 2 shows the initial conditions for differential equations.

C	1.5 μF/cm^2
G_L	0.15 mS/cm^2
V_r	– 65 mV
G_{NaP}	0.5 mS/cm^2
G_H	1.5 mS/cm^2
G_{Na}	52 mS/cm^2
G_K	11 mS/cm^2
E_{Na}	55 mV
E_K	– 90 mV
E_H	– 20 mV

Table 1. Parameters and constants used in computer simulations

$V(0)$	– 65 mV
$m_p(V)\|_{t=0}$	0.0155
$m_{hf}(V)\|_{t=0}$	0.1897
$m_{hs}(V)\|_{t=0}$	0.3106
$m(V)\|_{t=0}$	0.0062
$h(V)\|_{t=0}$	0.9895
$n(V)\|_{t=0}$	0.0467

Table 2. Initial values used in computer simulations

All differential equations are solved by the fourth-order Runge-Kutta method by using C++.

3.1 Subthreshold resonance oscillation

Consider the neuron model with *Nap* and *H* channels shown in Fig. 2.

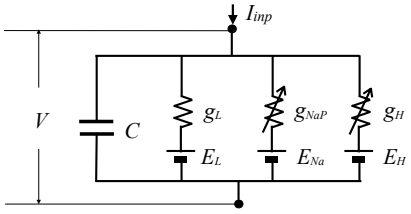

Fig. 2. A compartment neuron model with N_{aP} and H channels.

The following chirp current is given to this model as synaptic input.

$$I_{inp} = A_{inp}\ \sin(2\ \pi f\, t^{\,2}\ /T\ ) \quad (26)$$

Fig. 3 shows the membrane potential V and the amplitude and the phase of its FFT.

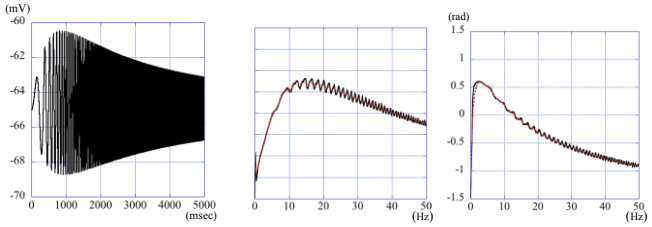

<Membrane potential> <FFT(amplitude)> <FFT(phase)

Fig.3. The membrane potential and the amplitude and the phase of its FFT. Units of horizontal lines are msec for the membrane potential, and Hz for FFT. Unit of vertical line is mV for the membrane potential.

From Fig.3, it is shown that the neuron model with *NaP* and *H* channels has the property of subthreshold resonance, that is, the band pass property. Its resonance frequency and the zero crossing frequency of the phase is around 13 Hz.

Fig. 4 shows affects of DC bias current to the subthresold resonance oscillation. Fixing the values of g_{NaP}=0.5mS/cm^2, g_H=1.5mS/cm^2, A_{inp}=1.5μA, f=30Hz, and T=5sec, results for id = 0μA, 0.25μA, and 0.5μA are shown in (a), (b), and (c), respectively.

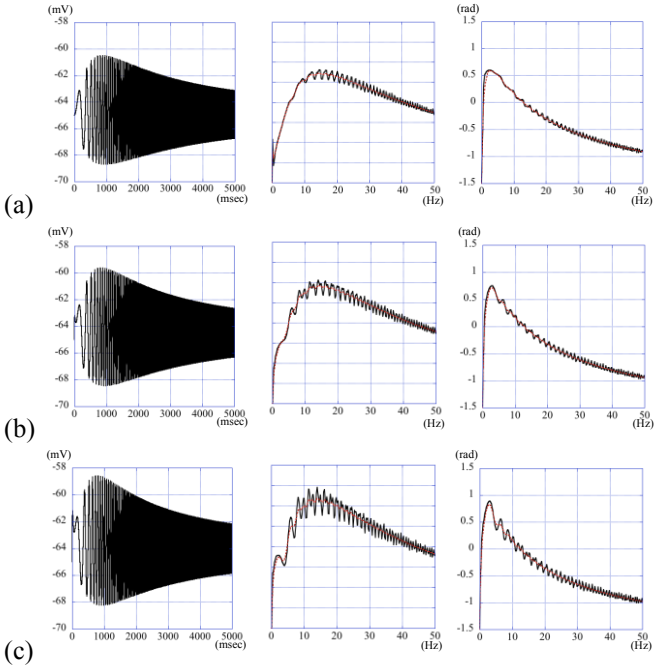

<Membrane potential> <FFT(amplitude)> <FFT(phase)

Fig.4. The membrane potential V and FFT amplitude and phase for various values of DC bias current: (a) id =0μA, (b) id = 0.75μA, and (c) id =1.5μA. Units are the same as Fig.3.

From Fig.4, as the value of id increases, the membrane potential moves to the more deporaralized potential side without change of its amplitude. For FFT, its amplitude tends to become sharp as id increases. But the property of the phase is no change.

3.2 Properties of Hodgkin-Huxley dynamics

In order to examine the generation of action potentials by giving a current input, the well known the Hodgkin-Huxley model with *Na* and *K* channels is considered. Its electrical circuit model is shown in Fig.5.

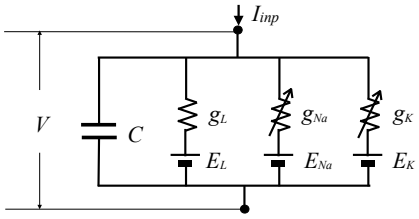

Fig.5. A Hodgkin-Huxley neuron model with N_a and K channels to generate the action potential.

3.2.1 Threshold voltage

The following input is given to the Hodgkin-Huxley dynamics, (14) to (24):

$$I_{inp} = id\ . \tag{27}$$

Fig.6 shows membrane potentials of the Hodgkin-Huxley dynamics with only DC bias current input.

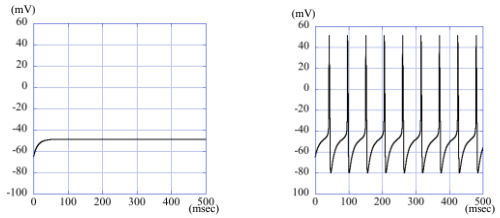

(a) (b)

Fig.6. Membrane potential: (a) is the result for id=2.2μA and (b) is the result for id = 2.5μA.

When id=2.2μA is given to the Hodgkin-Huxley dynamics, the membrane potential cannot exceed the threshold voltage, so action potential doesn't appear as shown in Fig.6(a). On the other hand, when id=2.5μA is given to them, the membrane potential can exceed the threshold voltage and then action potentials are generated as shown in Fig.6(b). For the case of parameter values in Table 1, it is estimated that the threshold voltage is approximately -48mV.

3.2.2 Effects of the frequency of an alternate current input

The following input is given to the Hodgkin-Huxley dynamics:

$$I_{inp} = A_{inp} \sin(2\ \pi f\ t). \tag{28}$$

Fig.7 shows membrane potentials of the Hodgkin-Huxley dynamics by giving only alternate current input with various frequencies, setting A_{inp}=2.5mS/cm^2 and id = 0.

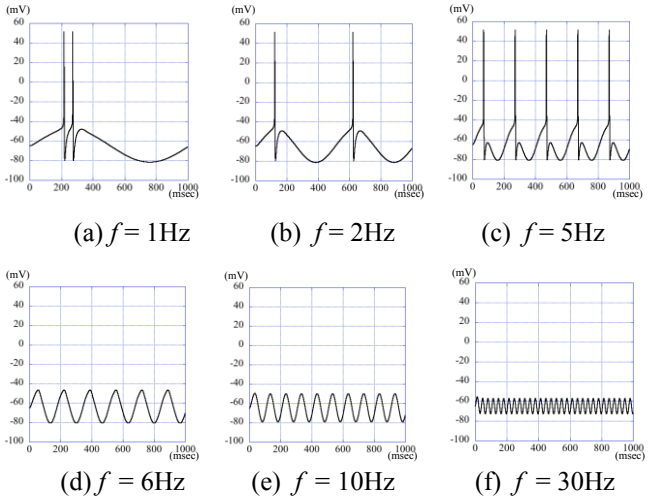

(a) f = 1Hz (b) f = 2Hz (c) f = 5Hz

(d) f = 6Hz (e) f = 10Hz (f) f = 30Hz

Fig.7. Membrane potential: By changing the frequency of alternate current input from 1Hz to 30 Hz, results are shown in (a) to (f) for the case of the described frequency.

Fig.7 shows the effects of the frequency of alternate current input to the generation of action potentials. A neuron has refractory period and cannot generate action potentials during this period even if its membrane potential exceeds the threshold voltage. For the case of 1Hz, the time change of alternate current input is relatively slow. So, the membrane potential remains high after refractory period of the first action potential and two action potentials are generated successively for the first positive cycle as shown in Fig.7(a). However, after the second action potential, the membrane potential drops and no more action potentials are generated owning to refractory period and the negative cycle of alternate current input. Up to f =5Hz, action potentials can be generated depending on the input frequency as shown in Fig.7(b) and (c). However, if the frequency becomes larger than 6Hz, action potentials cannot be generated because of the refractory period and a decrease in amplitude of the membrane potential even at the positive cycle of alternate current. Notice that the amplitude of membrane potential for alternate current input with higher frequency than 6Hz decreases as the frequency increases. The reason for this is the same as the above discussion.

3.2.3 Effects of DC bias current

As shown in Fig.7(d), alternate current with the frequency of 6Hz cannot generate action potentials. At the case like this, DC bias current may contribute to the generation of action potentials. Fig.8 shows the effects of DC bias current to the generation of action potentials. Setting A_{inp}=2.5mS/cm^2, simulations are made for f = 2Hz and 6Hz.

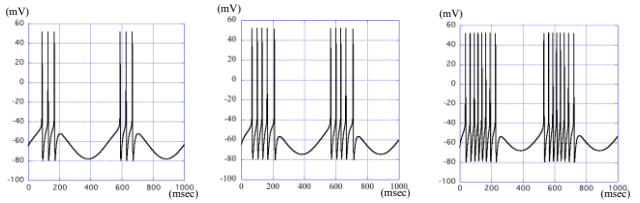

(a) *id*=0.5μA, 2Hz (b) *id*=1μA, 2Hz (c) *id* = 2μA,2Hz

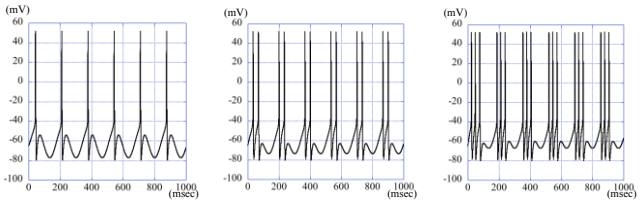

(d) *id*=0.5μA, 6Hz (e) *id*=1μA, 6Hz (f) *id* = 2 μA,6Hz

Fig.8. Membrane potential: By changing DC bias current to 0.5μA, 1μA, and 2μA for two frequencies of alternate current, 2Hz and 6Hz. Results for 2Hz are shown in (a), (b), and (c), and results for 6Hz are shown in (d), (e), and (f), respectively.

Comparison between Fig.7(a) and Fig.8(a), (b), and (c) suggests that a neuron tends to show burst firing as DC bias current increases. For the case of 6Hz, no action potential is generated for *id*=0 as shown in Fig.7(d). However, Fig.8(d) shows that action potentials can be generated by contribution of DC bias current. When DC bias current increases, a neuron can also show burst firing during positive cycle of alternate current input as shown in Fig.8(e) and (f).

3.3 Role of subthreshpold resonance for the generation of action potentials

By using the compartment model of Fig.1, we consider effects of the frequency of alternate current input and DC current input to the generation of action potentials. Fig.9 shows the results by changing both the frequency of alternate current input and the value of DC current, fixing A_{inp}=3.2 mS/cm^2.

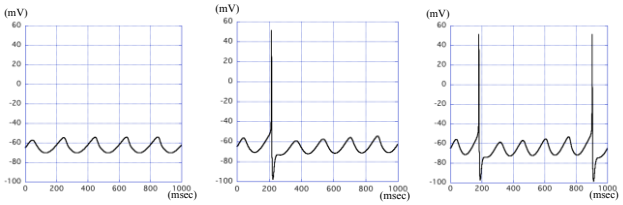

(a1) *id*=0, 5Hz (a2) *id*=0, 6Hz (a3) *id*=0, 7Hz

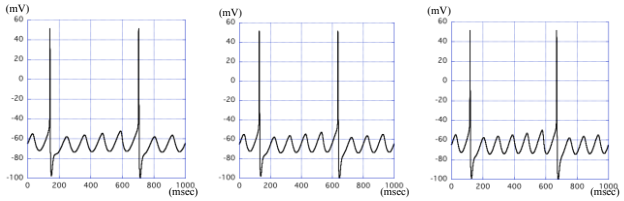

(a4) *id*=0, 9Hz (a5) *id*=0, 10Hz (a6) *id*=0, 11Hz

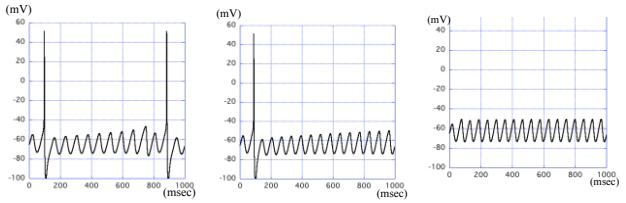

(a7) *id*=0μA,14Hz (a8) *id*=0μA,16Hz (a9)*id*=0μA,18Hz

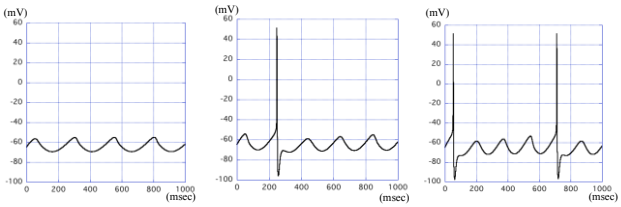

(b1)*id*=0.5μA,4Hz (b2)*id*=0.5μA,5Hz (b3)*id*=0.5μA,6Hz

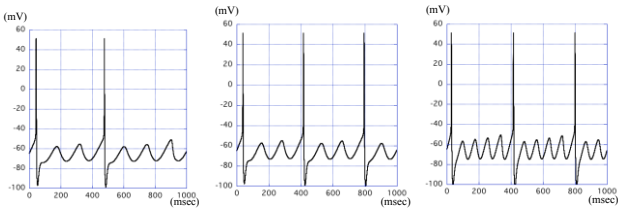

(b4)*id*=0.5μA,7Hz (b5)*id*=0.5μA,8Hz(b6)*id*=0.5μA,13Hz

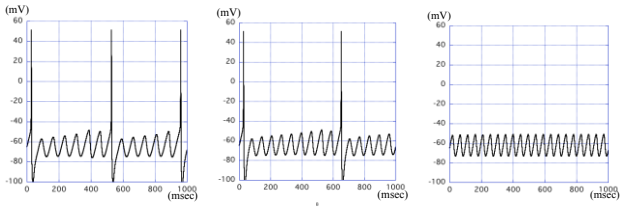

(b7)*id*=0.5μA,14Hz(b8)*id*=0.5μA,16Hz (b9)*id*=0.5μA,21Hz

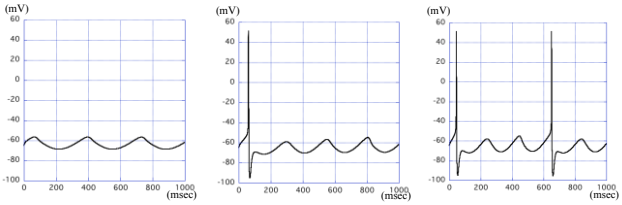

(c1) *id*=1μA, 3Hz (c2) *id*=1μA, 4Hz (c3) *id*=1μA, 5Hz

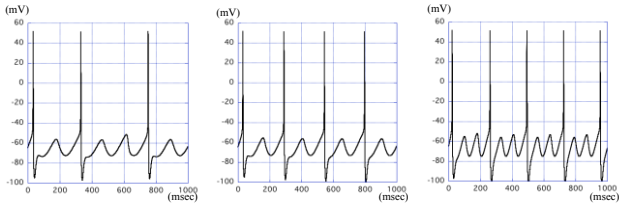

(c4) *id*=1μA, 7Hz (c5) *id*=1μA,8Hz (c6) *id*=1μA, 13Hz

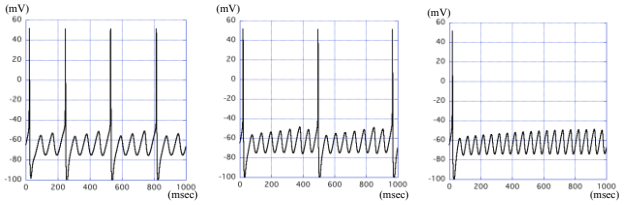

(c7) *id*=1μA, 14Hz (c8) *id*=1μA, 17Hz (c9) *id*=1μA, 20Hz

Fig.9. Membrane potential: By changing DC bias current with 0μA, 0.5μA, and 1μA and the input frequency, results are shown in (a1)-(a9), (b1)-(b9), and (c1)-(c9), respectively.

When id = 0μA, no action potentials are generated at the frequency smaller than 5Hz and greater than 18Hz. For the frequency between 7Hz to 14Hz, two action potentials are generated within one second, as shown in Fig.9 (a3)-(a7). However, for the frequency 10Hz, the interval between two action potentials has the minimum value (Fig.9 (a5)). At the frequencies 6Hz and 16Hz, only one action potential is generated. For the case of id = 0.5μA, no action potentials appear at the frequency smaller than 4Hz and greater than 21Hz. For the frequency between 8Hz to 14Hz, three action potentials are generated within one second, as shown in Fig.9 (b5)-(b7). However, the interval between action potentials has the minimum value at 13Hz(Fig.9 (b6)). At the frequencies 6Hz, 7Hz and 16Hz, only one action potential is generated. In the case of id = 1μA, no action potentials are generated at the frequency smaller than 3Hz and greater than 29Hz (data not shown). For the frequency between 8Hz to 14Hz, four action potentials are generated within one second, as shown in Fig.9 (c5)-(c7). At the frequencies 7Hz, 17Hz, 18Hz, and 19Hz, three action potentials are generated. On the other hand, one action potential appears at the starting positive cycle for 20Hz as shown in Fig.9 (c9). The reason for this may be that the fast rising of positive cycle of alternate current with 20Hz, one action potential can be generated owning to the large value of A_{inp}, that is, the membrane potential will reach into the threshold voltage quickly. Of course, the change of an activation variable $m(V)$ and an inactivation variable $h(V)$ in (8) and an inactivation variable $n(V)$ in (22) might be related to this phenomenon.

4. CONCLUSION

The neuron model with *NaP* channels and *H* channels has the property of the subthreshold resonance. By incorporating Hodgkin-Huxley dynamics into this model, we examined the relation between the subthreshold resonance oscillation and the generation of action potentials. By computer simulations, the frequency of alternate current input and DC bias current have an important role in the generation of action potentials, especially, burst firing. As the value of id increases, the maximum number of action potentials generated within one second increases, that is, two action potentials are generated for id = 0μA, three action potentials for id = 0.5μA, and four action potentials for id = 1μA. As shown in Fig.3, this neuron model has the resonance frequency around 13Hz. So, the maximum number of action potentials can be obtained around this ferequency by increasing id. However, in the case of id = 0μA, two action potentials can be generated at the frequency around 10Hz, which is a little bit smaller than the resopnance frequency. This suggets that the DC bias may adjust the timing of generation of action potentials, that is, the burst firing, which has a key role in higher information processins in our brain.

REFERENCES

Acker, C.D., Kopell, N., and White, J.A. (2003) Synchonization of strongly coupled excitatory neurons: Relating network behavior to biophysics. J. Computational Neuroscience, 15, pp/71-90

Agrawal, N., Hamam, B.N., Magistretti, J., Alonso, A, Ragsdale, D.S.(2001) Persistent sodium channel activity mediates subthreshold membrane potential oscillations and low-threshold spikes in rat entorhinal cortex layer V neurons. Neuroscience, Vol. 201, pp.71-90

Dickson, C.T., Magistretti, J., Shalinsky, M.H., Fransen, E., Hasselmo, M.H., and Alomso, A.(2000) Properties and role of I_h in the pacing of subthreshold oscillations in enrorhinal cortex layer II neurons. J. Neurophysiology, Vol. 83, pp.2562-2579

Gutfreund, Y., Yarom, Y. and Segev, I. (1995) Subthreshold oscillations and resonant frequency in guinea-pig cortical neurons. J. Physiol, Vol.483, pp.621-640

Haas, J.S. and White, J.A. (2002) Frequency selectivity of layer II stellate cells in he medial entorhinal cortex. J. Neurophysiol, Vol. 88, pp.2422-2429

Hutcheon, B., Miura, R.M., Yarom, Y. and Puil, E. (1994) Low-threshold calcium current and resonance in thalamic neurons: A model of frequency preference. J. Neurophysiol, Vol.71, pp.583-594

Johnston, D., Christie, B.R., Frick, A., Gray, R., Hoffman, D.A., Schexnayder, L.K., Watanabe, S. and Yuan, L.L. (2003) Active dendrites, potassium channels and synaptic plasticity. Phil. Trans. R. Soc. London B, Vol.358, pp.667-674

Kitajima, T. (2012) The property of subthreshold resonace observed in voltage-dependent ion channels. Conference of World Research & Innovation Convention on Engineering & Technology (WRICET2012), Keynote Address 3

Kitajima, T. and Feng, Z.G. (2013) Contribution of voltage-dependent ion channels to subthreshold resonance. 9th Asian Control Conferencc (ASCC 2013 Istanbul), WeD7

Kitajima, T. and Hara, K. (2000) A generalized Hebbian rule for activity-dependent synaptic modification. Newral Networks, Vol.13, pp.445-454

Koch, C. (1984) Cable theory in neurons with active linearized membrane. Biol. Cybern, Vol.50, pp.15-33

Lampl,I. and Yarom, Y (1993) Subthreshold oscillations of the membrane potential; A functional synchronizing and timing device. J. Neurophysiol, Vol.70, pp.2181-2186

Mauro, A., Conti, F., Dodge, F. and Shor, R. (1970) Subthreshold behavior and phe- nomenological impedance of the squid giant axon. J. Gen. Physiol, Vol.55, pp. 497-523

Narayanan, R. and Johnston, D. (2008) The *h* channel mediates location dependence and plasticity of intrinsic phase response in rat hippocampal neurons. J. Neurosci, Vol.28, pp.5846-5860

Puil, E., Meiri, H. and Yarom, Y. (1994) Resonant behavior and frequency preferences of thalamic neurons. J. Neurophysiol, Vol.71, pp.575-582

Richardson, M.J.E., Brunel, N., and Hakim, V. (2003) From subthreshold to firing-rate resonance. J. Neurophisilol, Vol. 89, pp.2438-2554